THE JOURNAL OF PHYSICAL CHEMISTRY A

 VOLUME 105, NUMBER 3, JANUARY 25, 2001

LETTERS

Water Dimers in the Atmosphere: Equilibrium Constant for Water Dimerization from the VRT(ASP-W) Potential Surface

Nir Goldman,[†] Raymond S. Fellers,[‡] Claude Leforestier,[§] and Richard J. Saykally*,[†]

Department of Chemistry, University of California, Berkeley, California 94720-1416, Yahoo!, 3420 Central Expressway, Santa Clara, California 95051, Laboratoire Structure et Dynamique des Systèmes Moléculaire et Solides (UMR 5636), CC 014, Université des Sciences et Techniques du Langue-doc, 34095 Montpellier Cédex 05, France

Received: September 29, 2000; In Final Form: November 20, 2000

The equilibrium constant for water dimerization (K_P) was determined as a function of temperature via rigorous calculation of the canonical $(H_2O)_2$ partition function using the recently developed split Wigner pseudospectral method and the VRT(ASP-W) pair potential. Our $K_P(T)$ values are significantly larger than those from previous theoretical treatments but somewhat smaller than literature experimental values, which exist, however, only over a very limited temperature range. These results indicate that water dimers can exist in sufficient concentrations (e.g., 10^{16} cm^{-3} at 40 °C and 100% relative humidity) to affect physical and chemical processes in the atmosphere.

Introduction

The role of water dimers in atmospheric processes is a controversial issue that has not been clearly resolved despite considerable effort. The excess absorption of solar radiation by the atmosphere has been ascribed to water dimers because these seem to be the only species present under most atmospheric conditions in sufficient densities to produce the measured effects.[1−3] However, recent measurements[2,4] have shown that the absorption of solar flux at dimer vibrational overtone wavelengths predicted in ref 2 is negligibly small.[1,4] Similarly, the water dimer has been proposed as the source of "the water continuum" absorption in the far-infrared.[5] Water dimers are also postulated to catalyze the formation of atmospheric H_2SO_4, and ab initio calculations have shown that the transition state of the $(H_2O)_2 + SO_3\cdot(H_2O)$ reaction is 0.7 kcal/mol lower than that for the isolated reactants.[6,7] This has been confirmed by experimental results which have shown the formation of H_2SO_4 from SO_3 to have a quadratic dependence on water vapor.[8,9] In addition, the abundance of water dimers in the atmosphere may be important for modeling water recondensation[10] and for the formation of radical complexes like $HO_2\cdot H_2O$, which have been predicted to exist in relatively high concentrations in the atmosphere.[11,12] Nevertheless, and despite various experimental and theoretical attempts, there remains considerable uncertainty in atmospheric water dimer concentrations,[2,3,13,14] primarily because neither rigorous models of the requisite water dimer potential nor rigorous methods for computing concentrations existed until very recently.[15,16]

Assuming rigid monomers, the water dimer potential is a six dimensional surface with a very complex topology, viz., eight identical global minima connected by three different low energy tunneling paths.[17] Many ab initio and empirical pair potentials have been published, but none is able to accurately describe the observed dimer properties.[18] Ab initio potentials suffer from basis set superposition error and/or poor convergence of the

* Corresponding author. E-mail: saykally@uclink4.berkeley.edu.
[†] University of California.
[‡] Yahoo!.
[§] Université des Sciences et Techniques du Langue-doc.

10.1021/jp003567a CCC: $20.00
Published on Web 12/15/2000

interaction energy, and empirical potentials are usually designed to mimic the bulk phase, which leads to poor estimations of the dipole moment and binding energy of the dimer. These problems have resulted in large discrepancies among published values of the water dimerization equilibrium constant versus temperature, $K_P(T)$.[2,10,19]

Here we determine $K_P(T)$ and subsequently the dimer partial pressure versus relative humidity, using the VRT(ASP-W) water pair potential recently determined from laser VRT spectroscopy.[16] The dimer tunneling splittings from hydrogen bond rearrangements and the intermolecular vibrational frequencies provide a highly sensitive probe of the complex water intermolecular potential energy surface (IPS),[20] and such measurements have been made extensively by our laboratory.[21−23] The VRT(ASP-W) potential was generated by fitting Stone's ASP-W form[24] to $(D_2O)_2$ microwave and far-IR transitions using a nonlinear least-squares regression procedure. The ASP-W potential has 72 parameters, but only four that correspond to anisotropic exchange-repulsion forces were actually varied in the fit.[16] VRT(ASP-W) is the most accurate water pair potential determined to date, although van der Avoird and co-workers have obtained one of comparable quality by "tuning" an ab initio potential derived from symmetry adapted perturbation theory.[25]

Determination of $K_P(T)$

The computationally demanding calculations of VRT states on the VRT(ASP-W) potential necessary to determine $K_P(T)$ were performed using the split Wigner pseudo-spectral (SWPS) approach,[15,26] which accurately and efficiently determines the eigenstates from a multidimensional version of a discrete variable representation (DVR).[27] In SWPS, the radial dependence of the potential is represented by a basis of sine functions and the angular part by Wigner functions. Improvements were made on the original SWPS code[15] by including the ARPACK Lanczos matrix package, which keeps the Lanczos vectors orthogonal so as to avoid possible ghost eigenvalues. The computational difficulties associated with such a 6D calculation are formidable. It was found that ca. 10 basis functions were needed per degree of freedom (6) in order to achieve acceptable accuracy. As a result, the Hamiltonian has ca. 10^{12} elements, and converging a partition function can take ca. 1 week of CPU time on a DecAlpha PC164 LX workstation with a 533 MHz Pentium II processor. In addition, storage of the Lanczos basis vectors, required to keep orthogonality, generally requires close to 512 MB memory. For our purposes, the grid size for the calculation was set to 16 radial functions and 19 radial points (with four points kept after H.E.G. optimization) over a range of 4−12 Bohr units, and j_{max} for the monomer was set to nine. This grid size and radial range were ultimately chosen because it adequately samples the VRT(ASP-W) potential without making the calculation of eigenstates too expensive. Convergence was estimated by increasing the radial grid to as large as 20 radial functions and 23 points over a range of 4−25 Bohr, and separately by extending the angular grid to as high as $j_{max} = 10$, wherein the equilibrium constant was found to not vary by more than 5%. This indicates that the chosen grid size and radial range is sufficient to accurately sample the potential surface.

Eigenvalues for $(H_2O)_2$ with $J = 0$ were calculated to energies near the dissociation limit, which was determined to be the lowest eigenvalue computed for the A_1^+ symmetry (ca. approximately -1085 cm^{-1} for the grid size and radial range used for our calculations). The water dimer was then assumed to be a prolate symmetric top, and the computed VRT eigenvalues were used to calculate a partition function in the canonical ensemble according to

$$Q_{dimer} = g(\mathrm{sym},J,K)\sum_n e^{-\beta E_n} \tag{1}$$

Here $g(\mathrm{sym},J,K)$ is the degeneracy due to the spin statistical weight of the symmetry for which the eigenstates have been calculated, and that due to the K and M levels for a prolate top, $\beta = k_B T$, and E_n are the computed eigenvalues. The spin statistical weights are well-known,[28] and the degeneracy for a prolate top is

$$\begin{aligned} g(J,K) &= (2J+1) \qquad \text{for } K = 0 \\ &= 2(2J+1) \qquad \text{for } K > 0 \end{aligned} \tag{2}$$

To efficiently compute the $J > 0$ energy levels for $(H_2O)_2$, the prolate top rotational energy level expression

$$F(J,K) = hc[BJ(J+1) + (A-B)K^2] \tag{3}$$

was used, where $F(J,K)$ is the rotational energy level correction to the computed eigenvalues, h is Plank's constant, and c is the speed of light. The rotational constants used are

$$A = 7.5919\ \mathrm{cm}^{-1} \qquad B = 0.2047\ \mathrm{cm}^{-1} \qquad C = 0.2039\ \mathrm{cm}^{-1}$$

which indicates that the prolate top approximation is quite accurate for lower values of J. The above rotational constants correspond to the $K_a' = 0$, A_1^+/B_1^- transition, and closely reflect the equilibrium geometry of the dimer. The measured B and C rotational constants vary by as much as 7.8%[22] with the VRT state, and using the highest values increased the partition function by approximately 8% relative to using the lowest values. To determine the convergence of the partition function, calculations were performed using eigenstates computed with the grid described above. An energy cutoff of 1000 cm^{-1} converged the partition function to better than 1%. We conservatively assume an overall convergence of 5%. It should be noted that due to the relatively poor convergence of E states, calculations were performed in which the E^+ states were substituted with the A_1^+ states and the E^- states were substituted with the A_2^- states, with the E state degeneracy correction applied to the substituted states. At a temperature of 85.4 °C, the calculation with substituted states agrees with the calculation with the E states included to within a deviation of 15%.

Once the dimer partition partition function has been determined, calculation of the dimerization equilibrium constant (K_2) follows from the canonical expression

$$K_2 = (Q_2/\lambda_2^{\,3})(Q_1/\lambda_1^{\,3})^{-2} \tag{4}$$

where Q_1 and Q_2 are the monomer and dimer partition functions, respectively, and

$$\lambda_i = h/(2\pi m_i k_B T)^{1/2} \tag{5}$$

where h is Planck's constant, k_B is the Boltzmann constant, and T is the absolute temperature.

The monomer partition function (Q_1) developed by Harris et al.[29] uses the VT2 linelist calculated by Viti and Tennyson[30] by performing explicit dynamics on the experimentally determined water monomer PJT2 potential energy surface of Polansky, Jensen, and Tennyson.[31] PJT2 was used to generate energy levels for all rotational states with up to $J = 35$, which resulted in a list of about 200 000 rotational−vibrational energy levels. The VT2 linelist is quite accurate in determining high energy

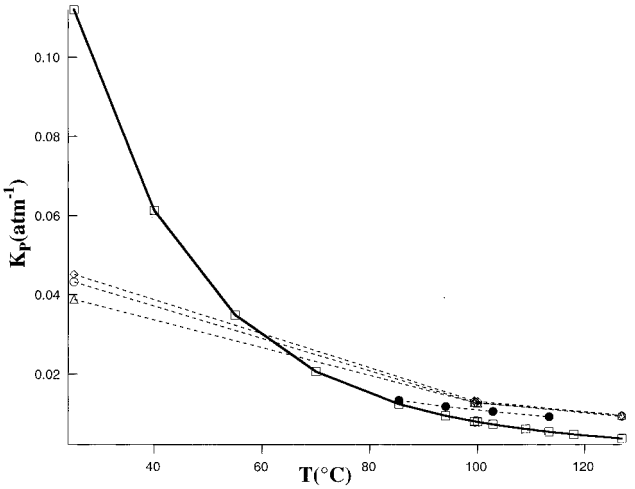

Figure 1. Temperature dependence of K_p using the monomer partition function developed by Harris et al. using the PJT2 monomer potential.[29] Comparison is made to Slanina et al.[38] and to Curtiss et al.[32] The solid line with unshaded squares corresponds to calculations also performed with the VRT(ASP-W) potential and using the PJT2 potential monomer partition function,[29] the dashed line with unshaded diamonds correspond to results from Slanina et al. using the MCYB pair potential, the unshaded circles corresponds to their results using the BJH/G pair potential, the unshaded triangles corresponds to their results using the MCY-B pair potential, and the dashed line with solid circles corresponds to the values measured by Curtiss et al. The small number of points from Curtiss et al. is due to the limited temperature range for which their experiments were performed. Extra points have been added in the plots of our calculations of the equilibrium constant in order to better display the exponential dependence of the curves. All of the calculations performed by Slanina et al. were done by finding the minimum of the potential by means of the analytic energy derivatives and then assuming a harmonic potential in its place. The measurements by Curtiss et al. of K_P were performed by using a modified thick hot wire cell and creating a voltage drop in the presence of H_2O vapor. The voltage drop varies according to $1/\lambda$, where λ is the thermal conductivity of the sample. Measurements were made by varying the temperature and pressure of the sample and recording the thermal conductivity. The dimerization equilibrium constants were then determined at various temperatures by fitting the thermal conductivity values to theoretical expressions for the thermal conductivity which contain the dimerization constant as a parameter (eq 3).

rovibrational states of the monomer because the PJT2 potential energy surface reproduced all of the experimentally determined energy levels with up to $J = 14$ known at the time of its construction to within a standard deviation of only 0.6 cm^{-1}. The values of Q_1 were plotted over a temperature range of 100−1500 K, and the resulting curve was fit via a least-squares fitting routine to a fifth order polynomial in order to obtain an analytical expression.

Results and Discussion

After the monomer and dimer partition functions had been determined, calculations of K_P were performed over a large range of temperatures and compared with previously published theoretical and experimental results (Figure 1). A large discrepancy between our results and those of Slanina et al.[10] is evident. This can be attributed to the fact that Slanina et al. used a simple harmonic potential to describe the dimer vibrations and did not account for quantum tunneling. Indeed, in a similar treatment, Suck et al.[13] predict a value of K_P at 23 °C of 4.9×10^{-3} atm^{-1}, compared to our value of 0.1229 atm^{-1} at the same temperature. Comparison of our K_p with those obtained by Curtiss et al.[32] via heat capacity measurements shows fortuitously good agreement. It is important to note that using their values for ΔH of dimerization, Curtiss et al. calculate a binding energy (D_e) of -22.761 ± 2.93 kJ/mol, which is considerably

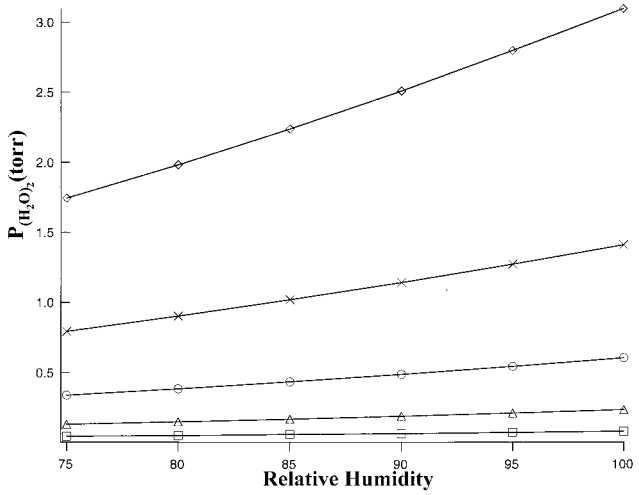

Figure 2. Comparison of $(H_2O)_2$ partial pressure vs relative humidity for temperatures from 25.15 to 85.4 °C. The squares correspond to a water dimer partial pressure profile at a temperature of 25.15 °C, the triangles correspond to $T = 40$ °C, the circles correspond to $T = 55$ °C, the ×'s correspond to $T = 70$ °C, and the diamonds correspond to $T = 85.4$ °C. All data points were calculated by first finding the water monomer vapor pressure by calculating the saturated water vapor pressure using a variant of the Clausius−Clapeyron equation, $P = P_0 e^{-H/RT}$, and then by multiplying by the relative humidity. The values of the constants used in the equation were $P_0 = 7.51 \times 10^8$ mmHg, $H = 42.8$ kJ/mol, and $R = 8.314$ J/(mol K). The dimer partial pressure was then found by taking the dimerization equilibrium constant calculated at each temperature and solving for the dimer partial pressure.

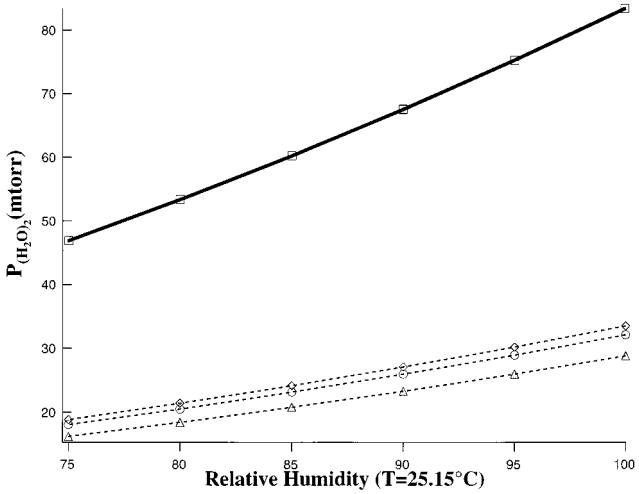

Figure 3. Dimer partial pressures vs relative humidity at $T = 25.15$ °C, comparing calculations performed by Slanina et al.[38] to our calculations performed with the VRT(ASP-W) dimer potential. All data points were calculated with the same method as in Figure 2. The solid line with unshaded squares corresponds to our values for the dimer partial pressure using the dimerization equilibrium constant calculated using the PJT2 monomer partition function,[29] the dashed line with unshaded diamonds corresponds to the dimer partial pressures derived from the results of Slanina et al. using the MCYB potential, the unshaded circles correspond to values derived from their results using the BJH/G potential, and the unshaded triangles correspond to the values derived from their results using the MCY−B potential. Once again it should be noted that the calculations of Slanina et al. were performed by finding the potential well bottom and making a harmonic approximation, which helps to explain the discrepancy between his results and ours.

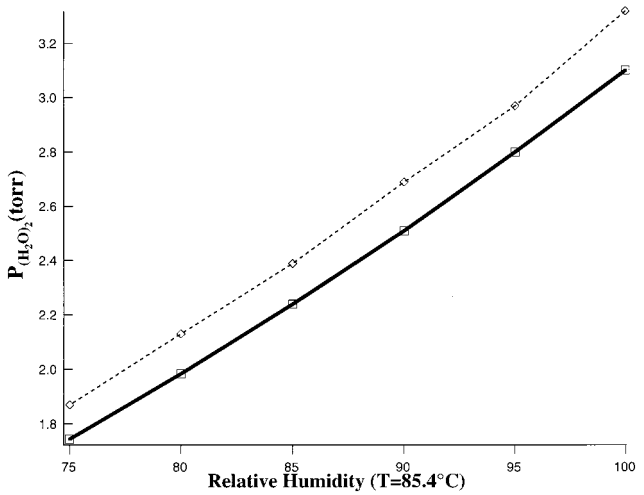

Figure 4. Dimer partial pressures vs relative humidity at $T = 85.4$ °C, comparing the results of Curtiss et al. to our calculations with the VRT(ASP-W) dimer potential. The dashed line with unshaded diamonds corresponds to the dimer partial pressure derived from the results of Curtiss et al. at $T = 85.4$ °C, and the solid line with unshaded squares corresponds to our results using the PJT2 monomer partition function. Again, it should be noted that the dimer partial pressure derived from the results of Curtiss et al. should be considered an upper limit to the actual answer at the above temperature.

higher than that found from either high level ab initio calculations (−20−21 kJ/mol)[33−36] or from our VRT(ASP-W) surface (−20.543 kcal/mol),[16] but again, a primitive approximation for the eigenstates was used to obtain their results. Hence, the K_P values measured by Curtiss et al. are an upper limit. Our results slightly underestimate the value of K_P due to the fact that as the highly nonrigid H_2O dimer accesses higher excited rotational states, the values of the rotational constants will decrease, causing a corresponding increase in K_P, and this effect is not included in our treatment. Again, experimenting with various grid sizes and ranges has shown that the equilibrium constant is relatively insensitive to the radial grid and range. For example, a calculation with a grid of 7 radial functions over a range of 3.5−9 au yields an equilibrium constant that differs from that of a grid of 20 radial functions over a range of 3.5−15 au by only 1.6% at a temperature of 85.4 °C. In any case, the agreement between our results and the experimental values determined by Curtiss et al. is reasonable (within a deviation of 7% at 85.4 °C) over the very narrow temperature range of 30 °C actually examined by them., but our calculations clearly span a much larger temperature range.

In addition, we have checked the above results calculated from the VRT(ASP-W) potential against those computed via the same method from the SAPT5s potential recently determined from similarly detailed ab initio calculations and VRT data by Groenenboom et al.[25] Eigenstate calculations were performed on both potentials using a grid size of 7 radial functions and $j_{max} = 6$ in order to gain some preliminary insight into the equilibrium constant predictions of both potentials. The results for K_P at a temperature of 65 °C agree to within a deviation of 5%.

We present the calculated dimer partial pressure vs relative humidity at several relevant temperatures in Figure 2. Again, Slanina et al. greatly underestimate the value of the dimer partial pressure (Figure 3) while Curtis et al. overestimate this quantity somewhat (Figure 4). At a temperature of 25 °C, we predict dimer partial pressures in the milliTorr region, whereas near 85 °C, this rises to several Torr. Thus, it is probable that the water dimer can be indeed present in the atmosphere in sufficient quantities to have significant effects on solar absorption, far-IR light propagation, the catalysis of H_2SO_4 formation, and on other atmospheric processes. The results presented here will allow these effects to be definitely assessed, when combined with the relevant radiative transfer and kinetic models.

The recent measurements of solar radiation absorption by Daniel et al.[1] and Hill and Jones[4] clearly show that water dimer absorption is not significant at visible-near-infrared wavelengths, corresponding to O−H vibrational overtone transitions. This, in turn, demonstrates that previous predictions[2,3,13] of dimer concentrations are seriously in error, as we indeed confirm here (Figure 3). Moreover, the predicted dimer absorption cross sections[2] must be too large by a similar factor, since those values combined with our predicted dimer concentrations would actually yield measurable absorptions. For example, Daniel et al. predict a water dimer optical depth of 0.02 on the day of their measurements. Using the atmospheric conditions of that day, their absorption cross section taken from Tso et al.,[37] and our estimate of the $(H_2O)_2$ concentration, we calculate an optical depth of approximately 0.3. This is not surprising, given the inadequate dynamical treatment and the poor dimer potential function used in their work. A correct treatment of the dimer O−H overtone absorptions would require a full 12-D treatment of the VRT dynamics, which is currently beyond the state of the art.

The dimer concentrations predicted here for high humidity conditions may be significant for several important chemical reactions, if not for absorption of sunlight. For example, in the marine boundary layer, where the water molecule density is 2.6×10^{17} molecules/cm^3 at the mean temperature of 10 °C,[11] the partial pressure of water dimers is 25.74 mTorr (0.27% total water, or 9.4×10^{14} dimers/cm^3). In the tropics at 80% relative humidity and 25 °C, the dimer partial pressure is 53.4 mTorr (0.23% of total water or 1.7×10^{15} dimers/cm^3). These concentrations can have significant effects on atmospheric reactions, e.g. for sulfuric acid formation.[6] Also, Francisco et al.[12] predict that up to 30% of atmospheric HO_2 may exist as the complex $HO_2 \cdot H_2O$, efficiently formed by the process:

$$(H_2O)_2 + HO_2 \rightarrow HO_2 \cdot H_2O + H_2O$$

Similar processes might occur for OH, and other radicals that form strong hydrogen bonds with water, such that the water complexes form a significant reservoir of these reactive species.

Acknowledgment. This investigation was supported by the Experimental Physical Chemistry program of NSF and the France-Berkeley Cooperative Grant Program.

References and Notes

(1) Daniel, J. S.; Solomon, S.; Sanders, R. W.; Portmann, R. W.; Miller, D. C.; Madsen, W. *J. Geophys. Res.-Atmos.* **1999**, *104*, 16785−16791.
(2) Chylek, P.; Geldart, D. J. W. *Geophys. Res. Lett.* **1997**, *24*, 2015−18.
(3) Pilewskie, P.; Valero, F. P. J. *Science* **1995**, *267*, 1626−1629.
(4) Hill, C.; Jones, R. L. *J. Geophys. Res.-Atmos.* **2000**, *105*, 9421−9428.
(5) Devir, A. D.; Neumann, M.; Lipson, S. G.; Oppenheim, U. P. *Opt. Eng.* **1994**, *33*, 746−750.
(6) Akhmatskaya, E. V.; Apps, C. J.; Hillier, I. H.; Masters, A. J.; Watt, N. E.; Whitehead, J. C. *Chem. Commun.* **1997**, 707−707.
(7) Loerting, T.; Liedl, K. R. *Proc. Natl. Acad. Sci. U.S.A.* **2000**, *97*, 8874−8878.
(8) Lovejoy, E. R.; Hanson, D. R.; Huey, L. G. *J. Phys. Chem.* **1996**, *100*, 19911−19916.
(9) Jayne, J. T.; Poschl, U.; Chen, Y. M.; Dai, D.; Molina, L. T.; Worsnop, D. R.; Kolb, C. E.; Molina, M. J. *J. Phys. Chem. A* **1997**, *101*, 10000−10011.

(10) Slanina, Z.; Crifo, J. F. *Int. J. Thermophysics* **1992**, *13*, 465−476.
(11) Aloisio, S.; Francisco, J. S. *J. Phy. Chem. A* **1998**, *102*, 1899−1902.
(12) Aloisio, S.; Francisco, J. S.; Friedl, R. R. *J. Phys. Chem. A* **2000**, *104*, 6597−6601.
(13) Suck, S. H.; Wetmore, A. E.; Chen, T. S.; Kassner, J. L., Jr. *Appl. Opt.* **1982**, *21*, 1610−14.
(14) Vaida, V.; Headrick, J. E. *J. Phys. Chem. A* **2000**, *104*, 5401−5412J Phys Chem a.
(15) Fellers, R. S.; Braly, L. B.; Saykally, R. J.; Leforestier, C. *J. Chem. Phys.* **1999**, *110*, 6306−6318.
(16) Fellers, R. S.; Leforestier, C.; Braly, L. B.; Brown, M. G.; Saykally, R. J. *Science* **1999**, *284*, 945−948.
(17) Smith, B. J.; Swanton, D. J.; Pople, J. A.; Schaefer, H. F.; III.; Radom, L. *J. Chem. Phys.* **1990**, *92*, 1240−7.
(18) Scheiner, S. *Annu. Rev. Phys. Chem.* **1994**, *45*, 23−56.
(19) Munoz-Caro, C.; Nino, A. *J. Phys. Chem. A* **1997**, *101*, 4128−35.
(20) Saykally, R. J.; Blake, G. A. *Science* **1993**, *259*, 1570−1575.
(21) Braly, L. B.; Cruzan, J. D.; Liu, K.; Fellers, R. S.; Saykally, R. J. *J. Chem. Phys.* **2000**, *112*, 10293−10313.
(22) Braly, L. B.; Liu, K.; Brown, M. G.; Keutsch, F. N.; Fellers, R. S.; Saykally, R. J. *J. Chem. Phys.* **2000**, *112*, 10314−10326.
(23) Busarow, K. L.; Cohen, R. C.; Blake, G. A.; Laughlin, K. B.; Lee, Y. T.; Saykally, R. J. *J. Chem. Phys.* **1989**, *90*, 3937−43.
(24) Millot, C.; Stone, A. J. *Mol. Phys.* **1992**, *77*, 439−462.
(25) Groenenboom, G. C.; Mas, E. M.; Bukowski, R.; Szalewicz, K.; Wormer, P. E. S.; van der Avoird, A. *Phys. Rev. Lett.* **2000**, *84*, 4072−4075.
(26) Leforestier, C.; Braly, L. B.; Kun, L.; Elrod, M. J.; Saykally, R. J. *J. Chem. Phys.* **1997**, *106*, 8527−44.
(27) Light, J. C.; Hamilton, I. P.; Lill, J. V. *J. Chem. Phys.* **1985**, *82*, 1400−9.
(28) Dyke, T. R. *J. Chem. Phys.* **1977**, *66*, 492−7.
(29) Harris, G. J.; Viti, S.; Mussa, H. Y.; Tennyson, J. *J. Chem. Phys.* **1998**, *109*, 7197−7204.
(30) Viti, S. Ph.D. Thesis, University of London, 1997.
(31) Polyansky, O. L.; Jensen, P.; Tennyson, J. *J. Chem. Phys.* **1996**, *105*, 6490−7.
(32) Curtiss, L. A.; Frurip, D. J.; Blander, M. *J. Chem. Phys.* **1979**, *71*, 2703−11.
(33) Xantheas, S. S. *J. Chem. Phys.* **1996**, *104*, 8821−4.
(34) Feyereisen, M. W.; Feller, D.; Dixon, D. A. *J. Phys. Chem.* **1996**, *100*, 2993−2997.
(35) Halkier, A.; Koch, H.; Jorgensen, P.; Christiansen, O.; Nielsen, I. M. B.; Helgaker, T. *Theor. Chem. Acc.* **1997**, *97*, 150−157.
(36) Mas, E. M.; Szalewicz, K. *J. Chem. Phys.* **1996**, *104*, 7606−14.
(37) Tso, H. C. W.; Geldart, D. J. W.; Chylek, P. *J. Chem. Phys.* **1998**, *108*, 5319−29.
(38) Slanina, Z.; Uhlik, F. *Int. J. Thermophys.* **1992**, *13*, 303−13.